A review of biochar toward carbon neutrality: Production optimization and carbon sequestration potential assessment

Pin Lv , Qun Huan , Min Song

PII: S3050-6603(26)00007-4
DOI: https://doi.org/10.1016/j.cnt.2026.100019
Reference: CNT 100019

To appear in: *Carbon Neutral Technologies*

Received date: 10 June 2025
Revised date: 20 January 2026
Accepted date: 4 March 2026

Please cite this article as: Pin Lv , Qun Huan , Min Song , A review of biochar toward carbon neutrality: Production optimization and carbon sequestration potential assessment, *Carbon Neutral Technologies* (2026), doi: https://doi.org/10.1016/j.cnt.2026.100019

Highlights

- Uncovering the key mechanism of biochar carbon sequestration efficiency: The coupling effect of feedstock (high carbon, low ash, low volatile matter) and pyrolysis process (temperature 500-600°C, residence time 120-180 min) was systematically elucidated as the key to achieve high carbon sequestration rate (>30%).
- Clarifying the core drivers of carbon sequestration: Through multiple regression analysis, biochar yield and total carbon content were identified for the first time as the most important drivers determining its carbon sequestration efficiency (CS).
- Quantifying the carbon benefits of multi-sector applications:
  Iron and steel smelting: Biochar application can achieve >20.3% carbon reduction.
  Building materials: 5% biochar blending can have a significant carbon negative effect (541-980 kg CO_2eq/t).
  Soil improvement: applying 20-40 t-ha-^{1} of biochar can significantly increase soil organic carbon stock by 26-30%, highlighting its potential as a soil carbon sink.
- Innovative construction of carbon sequestration prediction model: Successful application of machine learning (Random Forest, Neural Network) model reveals for the first time the complex non-linear influence of parameters such as pyrolysis temperature, total carbon, fixed carbon, volatile matter, ash and specific surface area on carbon sequestration rate, which provides a data-driven tool for targeted preparation.
- Suggest key future research directions:
  Multi-objective optimization models need to be developed to synergistically optimize the carbon benefits of biochar (carbon sequestration and emission reduction) with its functional needs in agriculture, construction, and other fields.
  There is a need to expand the data base of the models to improve their generalization and interpretation ability in terms of feedstock diversity and parameter scales.

A review of biochar toward carbon neutrality: Production optimization and carbon sequestration potential assessment

Pin Lv [a] ,Qun Huan [a] , Min Song [a,*]

[a] *Key Laboratory of Energy Thermal Conversion and Control of Ministry of Education, School of Energy and Environment, Southeast University, Nanjing, Jiangsu 210096, China*
** Corresponding author: Min Song*
Tel: +86-13770606581; Fax: +86-025-83790986
E-mail address: minsong@seu.edu.cn

Abstract

Biochar, as a prominent carrier of carbon-negative technology, plays a pivotal role in achieving the Dual Carbon Goals through its preparation process and carbon sequestration mechanisms. This review synthesizes literature on how feedstock properties (C, Ash, VM) and pyrolysis parameters (temperature, residence time) jointly influence the carbon sequestration efficiency of biochar. The literature indicates that carbon sequestration (CS) rates exceeding 30% can be attained using high-carbon, low-ash feedstocks at pyrolysis temperatures ranging from 500 to 600 ℃ and residence times between 120 and 180 minutes. We summarize reported findings showing that yield and total carbon content are the primary factors driving carbon sequestration. We also summarize carbon benefits of biochar across several typical application scenarios: a 17-23% reduction in carbon emissions in steelmaking (depending on the biochar substitution ratio); a carbon-negative effect of 541-980 kg CO_2 eq/t when blending 5% biochar into construction materials, and an enhancement in organic carbon storage by 26-30% when applying 20-40 $t \cdot ha^{-1}$ of biochar to soil. Furthermore, reported machine learning models (random forest and neural network) reveal the nonlinear effects of pyrolysis temperature, total carbon, fixed carbon, volatile matter, ash content, and specific surface area on the carbon sequestration rate. This research provides a theoretical foundation and technical support for the targeted preparation of biochar, clarifying its sequestration mechanisms and its potential low-carbon applications across various fields.

Keywords： Biochar; Pyrolysis; Carbon sequestration; Steelmaking; Building materials;

Soil ; Machine learning

1 Introduction

The global climate system is undergoing profound transformations characterized by warming trends. In response to this crisis, the Intergovernmental Panel on Climate Change (IPCC) has established a non-negotiable target of limiting global temperature rise to 1.5 ℃ [1]. Anthropogenic greenhouse gas emissions – with CO_2 constituting the primary driver – account for over 60% of increased radiative forcing. This establishes decarbonization as the central focus of global climate mitigation strategies [2]. Aligning with this scientific consensus, signatories to the Paris Agreement have committed to carbon neutrality timelines, including China's Dual Carbon Goals (carbon peaking by 2030, carbon neutrality by 2060) [3]. Nevertheless, conventional emission reduction approaches face dual constraints of technological limitations and economic feasibility, necessitating urgent development of efficient negative emission technologies and advanced carbon sequestration vectors [4].

Biomass exhibits a significantly lower contribution to atmospheric CO_2 accumulation compared to fossil fuels. At the same time, its renewable nature constitutes a fundamental distinction that provides inherent cost-effectiveness for developing carbon sequestration materials like biochar [5]. Direct biomass combustion re-releases carbon, maintaining a closed carbon cycle. In contrast, biochar sequesters carbon permanently, creating a carbon-negative pathway from atmospheric CO_2 to solid carbon [6]. Through synergistic carbon sequestration and resource regeneration mechanisms, biochar presents a climate solution that concurrently addresses economic viability and technical feasibility for achieving carbon neutrality goals [7,8]. In this review, biochar consistently refers to solid carbon derived from thermochemical conversion of lignocellulosic biomass. While traditionally applied to soil uses, the term is broadly adopted here to cover steelmaking and construction materials, acknowledging that specifications vary by application. All forms, however, share a common feedstock and carbon-negative potential.

Importantly, the biomass used for biochar production is highly diverse in both source and supply-chain setting. In addition to agricultural and forestry residues, many

recent biochar initiatives draw on a broad range of organic waste streams (e.g., urban green waste, food-processing and kitchen residues), indicating a growing integration of carbon removal with waste management and circular-economy strategies [9]. This diversity goes beyond availability: feedstock-dependent differences in ash/mineral content, elemental composition, and possible contaminants can affect biochar yield, stability, and end-use constraints, and ultimately shape key performance indicators and life-cycle carbon budgets under a consistent assessment benchmark [10]. Spatially explicit assessments spanning multiple feedstock categories suggest that both feedstock type and spatial distribution strongly influence negative-emission potential, costs, and practical deployment priorities [11].

Thermochemical conversion technologies (pyrolysis, hydrothermal carbonization) transform unstable organic carbon in agricultural and forestry waste into stable biochar materials. The resulting hierarchical pore networks and abundant surface functional groups endow biochar with dual carbon sequestration mechanisms: physical adsorption and chemisorption [12]. Its highly carbonized aromatic-alkyl composite structure contributes significantly to emission reduction. Global modeling projections indicate that scaled biochar deployment could achieve an annual carbon mitigation potential of 1.0 Gt CO_2e by 2050, simultaneously establishing a closed-loop decarbonization system through enhanced carbon sequestration efficiency [13]. Nevertheless, the life-cycle carbon budget of biochar—from production to degradation—exhibits high variability due to coupled influences of feedstock provenance, pyrolysis parameters, and environmental responses. The absence of standardized quantitative assessment frameworks for sequestration efficacy across diverse application scenarios necessitates urgent development of multiscale carbon flow regulation theory [14]. Carbon sequestration (CS) refers to the amount of carbon that remains stored in biochar after pyrolysis, as opposed to being released back into the atmosphere. This value is calculated by measuring the carbon content in the biochar and comparing it with the carbon content in the original feedstock before pyrolysis [15]. The CS value is influenced by feedstock properties such as carbon content, ash content, and volatile matter, as well as pyrolysis conditions including temperature and residence time.

Recent years have witnessed a significant increase in biochar research. As demonstrated by data from the Web of Science Core Collection (Figure 1), publications have risen at an annualized rate of 23.72% from 2015 to 2024. Notably, only 473 articles explicitly addressed carbon emission implications, highlighting a critical research gap that motivates the present review. Research domains have expanded beyond traditional soil applications, demonstrating significant potential in engineering materials, composting, and blast furnace Steelmaking. However, investigations into its carbon emission implications remain limited (Only 473 results). Consequently, a comprehensive assessment of biochar's carbon sequestration potential necessitates further examination of its priming effects. Simultaneously, divergent physicochemical requirements across construction, metallurgy, and agriculture sectors demand integrated system analyses evaluating material properties, environmental impacts, and economic viability for accurate carbon sequestration assessment.

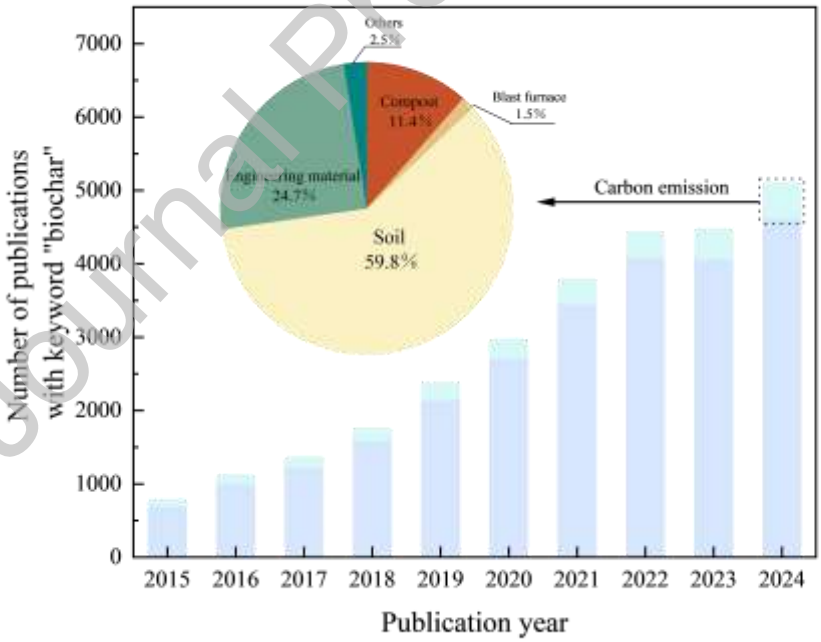

Fig. 1. Number of articles with biochar as a keyword during 2015-2024.

As a core vector within negative emission technology systems, research on chain-wide carbon regulation mechanisms of biochar holds strategic significance for

advancing global carbon neutrality. Although existing studies have made progress in optimizing individual processes, the cross-scale coupling effects among feedstock, process, and sequestration scenarios remain inadequately characterized. This review provides an overview of the carbon sequestration mechanisms and mitigation potential of biochar across the preparation, modification, and application chain. From the perspectives of feedstock selection and pyrolysis optimization, we elucidate key parameters governing carbon emission regulation while evaluating the multidimensional carbon benefits in steel production, construction materials, and soil applications. Finally, we develop machine learning models to predict carbon sequestration rates and interpret feature importance. Through this multiscale investigation, we aim to provide scientific support for scaling biochar technology and designing pathways to carbon neutrality. To ensure methodological consistency, all sequestration and decarbonization results discussed in this review are interpreted under a unified benchmark framework. The 100-year Global Warming Potential (GWP100) is adopted as the climate metric, with functional units defined as per ton of dry biomass (production), per ton of steel (Steelmaking), per ton of concrete (construction), and per hectare year (soil application).

2 Carbon Emission Regulation in Biochar Preparation

Although traditional biomass carbon sequestration pathways temporarily fix atmospheric CO_2, their organic carbon components remain susceptible to microbial mineralization during natural degradation, ultimately releasing carbon as CO_2 or CH_4 back to the atmosphere. To address this carbon cycle limitation, pyrolysis technology reconstructs biomass organic carbon into solid, liquid, and gaseous carbonaceous products [16]. Biochar—the carbon-rich solid residue from biomass pyrolysis—exhibits high carbon content and structural stability. Optimizing pyrolysis conditions (temperature, heating rate, residence time) significantly influences biochar yield and quality, thereby regulating carbon partitioning among phases [17]. Beyond biochar, pyrolysis concurrently generates liquid byproducts and gaseous products. Syngas produced during pyrolysis consists of key components, including CO_2, CO, CH_4, and

trace VOCs, each contributing differently to carbon reduction. While CO and CH_4 can be utilized as fuels to reduce net carbon emissions, CO_2 is a greenhouse gas that requires capture or management [18]. Efficient carbon sequestration strategies must optimize the recovery of CO and CH_4 for energy, while managing CO_2 emissions to maintain a carbon-negative process.

2.1 Raw material properties

In this review, biomass refers specifically to lignocellulosic agricultural and forestry residues (e.g., crop straws, wood residues, branches, forest litter). Biowaste such as municipal solid waste, sewage sludge, and livestock manure is excluded unless otherwise noted. Biomass is defined as organic material synthesized by photosynthetic organisms. All proximate (fixed carbon, volatile matter, and ash content) and ultimate (total carbon, hydrogen, oxygen, and nitrogen) analyses of biomass and biochar reported in this study are expressed on a dry basis, consistent with the standard methodology described by Lehmann and Joseph [15]. Unless otherwise specified, all data have been normalized to exclude moisture content to ensure comparability across different feedstocks and pyrolysis conditions. The regression analysis presented later in this paper is also based on these dry-basis values to maintain consistency throughout the dataset.

Biomass constitutes organic material synthesized by photosynthetic organisms through assimilation of atmospheric CO_2, water, and minerals. This heterogeneous assemblage encompasses plant-derived organics, microorganisms, their metabolites, and animal-derived organic waste, fundamentally representing chemically stored energy in organic carbon chains [19]. Consistent with this scope, we focus on lignocellulosic biomass. References to biochar in steelmaking or construction denote a common feedstock origin, without implying identical performance to soil applications. Identifying specific biomass types is crucial for efficient utilization. Despite significant compositional and spatiotemporal variations, biomass shares feedstock commonality for biochar production. Based on composition and origin, biomass is broadly classified as Lignocellulosic biomass: Primarily agricultural and forestry residues (post-harvest

crop straws, wood processing debris, naturally shed branches, forest litter); Non-lignocellulosic biomass: Mainly municipal solid waste (food waste, sewage sludge, concentrated livestock manure) [20]. Lignocellulosic biomass is preferred for biochar production due to its high carbon density, low moisture, and low contaminants, enabling efficient pyrolysis with higher yield and greater stability [12]. Lignocellulosic biomass is preferred for biochar production due to its low moisture content, high carbon density, and minimal contaminant levels, significantly outperforming non-lignocellulosic alternatives, which exhibit heavy metal accumulation risks, heteroatom-containing contaminants, and elevated processing costs [21]. Consequently, this study focuses exclusively on lignocellulosic biomass systems.

The carbon conversion efficiency and stability of lignocellulosic biomass during pyrolysis stem fundamentally from its unique physicochemical property matrix: highly developed porosity, exceptional specific surface area, carbon-enriched aromatic matrix, surface-active site distribution, and prominent cation exchange capacity [14]. These characteristics originate not only from processing conditions but are intrinsically governed by feedstock composition. Carbon content, ash, and volatile matter directly determine biochar yield and properties during pyrolysis, consequently influencing the total life-cycle carbon emissions [2]. The intrinsic cellulose – hemicellulose – lignin composition also shapes pyrolysis behavior: cellulose and hemicellulose decompose rapidly at lower temperatures with higher volatile release, whereas lignin, rich in aromatic carbon, favors stable char and long-term sequestration [17]. As most datasets lack detailed cellulose fraction data or correlations with sequestration efficiency, this factor was excluded from the regression modeling but noted for future refinement.

Biomass selection, therefore, plays a crucial role in defining biochar characteristics. Only through understanding parameter-specific impacts can biochar with tailored properties be produced. As summarized in Table 1, high carbon-sequestration feedstocks (CS > 30%) universally exhibit high yield (>40%), elevated total carbon content (>45 wt%), and low ash (<15 wt%). Conversely, low-carbon feedstocks (CS < 26%) are constrained by either high ash content (waste paper: 26.3 wt% ash) or low yield (rice straw: 28.1% yield), necessitating targeted optimization of

process parameters and feedstock blending strategies. For Table 1, additional descriptors (e.g., moisture, cellulose/hemicellulose/lignin fractions, heating value, trace metals) were considered but inconsistently reported across studies, with heterogeneous methods, units, and frequent missing data. To ensure comparability and avoid imputation bias, only consistently available parameters (TC, VM, Ash, pH, Yield, CS) were retained, aligning the table with the scalable evidence base.

Table 1
Chemical composition of different feedstocks [14,15,16,19,20].

Biomass	TC (%)	VM (%)	Ash (%)	pH	Yield(%)	CS (%)
Waste paper	56.0	30.0	53.5	9.9	36.6	24.7
Sawdust	75.8	17.5	9.9	10.5	28.3	28.5
Grass	62.1	18.9	20.8	10.2	27.8	28.0
Peanut shell	73.7	16.0	10.6	10.5	32.0	34.4
Chlorella	39.3	29.3	52.6	10.8	40.2	33.0
Waterweeds	25.6	32.4	63.5	10.3	58.4	47.1
Wheat straw	63.7	17.6	18.0	10.2	29.8	26.4
Poplar twigs	75.3	29.9	9.9	9.7	30.1	27.2
Poplar bark	72.7	30.5	11.4	9.3	34.3	30.4
Poplar leaves	55.6	28.4	27.1	10.6	36.6	26.7
Rice straw	60.6	28.9	22.5	11.5	33.4	25.9

(TC, Total Carbon; VM, Volatile Matter; CS, Carbon Sequestration—Biochar produced at 500 °C.)

Biomass selection, therefore, plays a crucial role in defining biochar characteristics. Only through understanding parameter-specific impacts can biochar with tailored properties be produced. As summarized in Table 1, high carbon-sequestration feedstocks (CS > 30%) universally exhibit high yield (>40%), elevated total carbon content (>45 wt%), and low ash (<15 wt%). All data in Table 1 were obtained under a pyrolysis temperature of 500 °C, ensuring comparability across feedstock types. Conversely, low-carbon feedstocks (CS < 26%) are constrained by either high ash content (waste paper: 26.3 wt% ash) or low yield (rice straw: 28.1% yield), necessitating targeted optimization of process parameters and feedstock blending strategies.

Based on Table 1 data, a multiple linear regression model predicting carbon sequestration rate (CS) was fitted, demonstrating robust explanatory power (R^2 =0.901).

Regression analysis (Figure 2) indicates carbon sequestration (CS) is jointly influenced by feedstock traits: yield strongly enhances retention; TC is positive but offset by VM and Ash, which reduce CS through volatilization and mineral inhibition. To reduce reporting bias, correlations were based on a harmonized subset and are presented as indicative rather than causal [13]. While pyrolysis temperature dominates surface area and acidity [22], our interpretation now emphasizes the multi-parameter coupling among yield, TC, VM, and Ash in governing CS, rather than a primary reliance on TC alone. Thus, feedstock screening should prioritize high-TC, high-yield, low-ash materials (peanut shells, Chlorella vulgaris), enhancing yield through pyrolysis parameter control; for high-ash feedstocks (waste paper), pretreatment modification or co-pyrolysis blending is required.

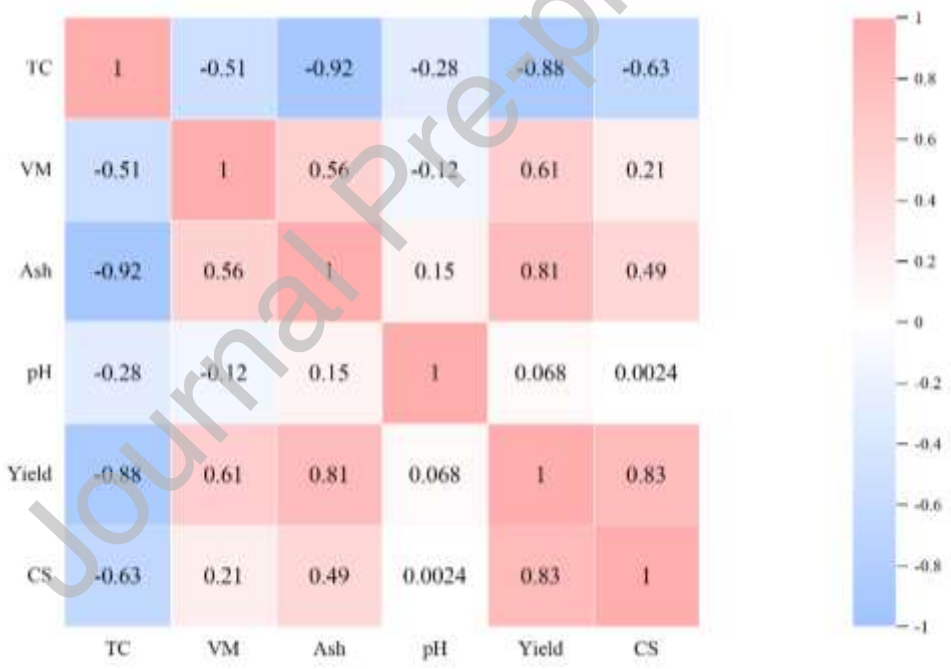

Fig. 2. Heat map of correlation matrix for different feedstock properties.

2.2 Pyrolysis parameters

The formation mechanisms of biochar properties exhibit significant dual dependency: constrained by the physicochemical characteristics of biomass feedstocks on one hand, and correlated with pyrolysis process parameters (heating rate, final

temperature, residence time) on the other. Pyrolysis temperature critically shapes biochar's sequestration performance: higher temperatures (500-600 °C) enhance carbonization, stability, and sequestration efficiency [20]. Lower temperatures (below 400 °C) produce biochar with lower carbon content and less stability, reducing its ability to sequester carbon in the long term [17]. Prolonged residence time enhances biochar yield through intensified polymerization of carbon skeletons, while the synergy of high temperatures and brief residence facilitates rapid volatilization and recombination of volatile matter, thereby promoting bio-oil formation [7]. Consequently, a balance must be struck between enhancing biochar quality and reducing greenhouse gas emissions. Optimizing pyrolysis conditions (temperature, heating rate, residence time) significantly influences biochar yield and quality, regulating carbon partitioning among phases [23]. Slow pyrolysis, typically at 300-550 °C with heating rates <0.8 °C·min^{-1} and residence times from minutes to hours, is widely regarded as the optimal method for maximizing biochar yield. This process maximizes biochar yield through secondary char formation during prolonged residence [24]. For slow pyrolysis, peak treatment temperature and residence time most substantially impact resultant biochar properties, determining its future carbon sequestration performance and application viability [20].

Pyrolysis atmosphere is critical: inert gases (N_2, Ar) favor high yields and stable pores; CO_2 or steam enhance porosity but lower carbon retention; limited oxygen promotes rearrangement yet reduces sequestration. Owing to scarce standardized data, this factor was excluded from regression modeling but qualitatively acknowledged.

2.3 Pyrolysis temperature

Temperature influences pyrolysis reactions by governing the distribution of solid, liquid, and gaseous products, thereby determining biochar yield and properties. At lower temperatures (300-400 °C), volatile matter is released more gradually, resulting in relatively higher proportions of bio-oil but lower solid carbon retention. From a carbon emission perspective, reduced CO_2 emissions offer advantages for greenhouse gas control. Within the medium-high temperature range (500-600 °C), pyrolysis

accelerates significantly, enhancing carbon retention rates as organic volatiles undergo thorough cracking. Concurrently, CO_2 emissions increase substantially, imposing greater environmental burdens [25]. Elevated temperatures (⩾500 °C) increase carbon stability, aromatization, and pore volume, promoting long-term sequestration but reducing nutrient availability [26]. Table 2 summarizes pyrolysis products and the corresponding carbon sequestration performance of straw-based biomass across different temperatures. In addition to the values reported in the literature, the carbon sequestration values for biochar that are not explicitly mentioned are calculated based on the method described in reference [27].

Table 2

Carbon sequestration rate of biochar at different pyrolysis temperatures.

TP (°C)	Biochar (%)	Bio-oil (%)	Syngas (%)	CS(%)	References
200	99.3	0.5	0.2	40.7[a]	[27]
350	52.5	35.0	10.0	45.3[a]	[27]
450	18.2	54.0	28.0	10.9[b]	[28]
489	19.2	42.0	32.0	13.7[b]	[29]
500	24.5	44.9	24.1	20.6[b]	[30]
530	26.1	51.0	22.0	18.5[b]	[31]
542	20.6	44.0	36.0	20.1[b]	[29]
595	22.2	46.0	40.0	24.1[b]	[29]
600	34.3	32.5	29.0	38.3[b]	[32]
650	26.8	20.0	50.0	34.1[a]	[27]

(TP, Temperature; CS, Carbon Sequestration—All data in this table refer to biochar produced from straw; [a]CS directly reported in Ref. [27]; [b]CS calculated using the method described in Ref. [27].)

Research on the relationships among carbon sequestration, bio-oil, syngas, and biochar reveals that temperature elevation promotes char formation and stability, thereby enhancing carbon sequestration. Bio-oil yield peaks at 350-400 ℃ while char yield and carbon sequestration capacity remain relatively low; balanced product distribution occurs at 530-550 ℃, enabling multi-purpose utilization; optimal carbon sequestration performance emerges at 500-600 ℃ with elevated biochar and gas yields but diminished bio-oil production, favoring carbon sequestration applications. The

incremental gain in carbon sequestration diminishes progressively with rising temperature, with the most significant increase occurring primarily within the 350-500 ℃ range [33]. To optimize the balance between carbon emissions and biochar quality, a stepwise pyrolysis protocol can be implemented. Through in-depth analysis of feedstock properties, a staged temperature program is designed: initial low-temperature treatment (300-400 ℃) removes volatile components while preserving carbon matrices, followed by medium-high temperature pyrolysis (500-600 ℃) to crack residual organics. This approach effectively controls carbon emissions, simultaneously retaining high-carbon biochar and suppressing peak greenhouse gas emissions.

2.4 Reaction residence time

Residence time duration critically determines the ultimate quality of pyrolysis products and carbon emissions. While prolonged residence facilitates stable biochar structure formation, it reduces carbonaceous material yield. Conversely, shorter residence times result in incomplete initial biomass decomposition, leaving tar components under-cracked and generating secondary emissions. This not only compromises product purity but also complicates emission control, imposing additional carbon mitigation challenges [34].

Table 3

Specific surface area at different residence time and temperature.

Biomass	TP (°C)	RT (min)	pH	Bet(m^2g^{-1})	References
Corn stover	650	15	10.50	43.40	[35]
Paper	500	120	8.78	47.42	[36]
Peanut shell	700	180	10.57	448.20	[37]
Pine wood	500	30	8.70	380.00	[38]
Rice husk	500	120	7.99	230.91	[39]
Rice straw	600	180	9.70	156.20	[40]
Wheat straw	600	180	9.10	183.30	[40]
Wood bark	500	30	9.80	350.00	[41]
Peanut shell	500	120	10.32	7.53	[42]
Corn cobs	500	60	10.16	477.00	[43]
Corn stalk	280	60	9.64	11.18	[44]
Walnut shell	260	60	9.40	9.43	[45]
Mango pit	400	120	10.34	29.14	[46]
Waste wood	240	60	9.14	25.74	[47]

(TP, Temperature; RT, Retention Time.)

Residence time is a key factor influencing the formation of biochar pore structure, but its effect requires comprehensive consideration combined with feedstock characteristics and pyrolysis temperature. Data in Table 3 show that under high-temperature and long-duration conditions (700 °C /180 min), peanut shell achieved a specific surface area of 448.2 m^2 /g, indicating a synergistic effect between temperature and time. For comparison, rice and wheat straw showed more limited pore expansion under identical conditions due to their higher silica content. In contrast, rice and wheat straw under the same temperature and time (156-183 m^2 /g) exhibited limited pore expansion due to their higher silica content. Generally, within the residence time range of 120-180 min, a relatively optimal combination can be achieved between biochar quality, energy efficiency utilization, and carbon emission control. Within this interval, a relatively stable carbon structure of the biochar is ensured while avoiding the undesirable outcomes associated with excessively short or long residence times, enabling efficient and low-carbon operation of the pyrolysis process.

2.5 Properties of Biochar

The carbon sequestration performance of biochar is significantly influenced by its physical and chemical structural characteristics, among which specific surface area and surface functional groups are the two most critical parameters [18]. Specific surface area is a key parameter governing the overall performance of carbonaceous materials. Biochar requires additional properties to compensate for lower specific surface areas, enabling it to exhibit reactivity comparable to conventional carbonaceous materials [48]. A larger specific surface area provides biochar with more reaction sites and adsorption zones, thereby enhancing its capacity to fixate greenhouse gases such as carbon dioxide. Particularly in biochars rich in micropores (<2 nm) and mesopores (2-50 nm), CO_2 molecules can be stably embedded within the pore structure through physical adsorption, delaying their release into the atmosphere. Surface functional groups on biochar, such as carboxyl (–COOH), hydroxyl (–OH), phenolic hydroxyl (–ArOH), and aldehyde (–CHO) groups, can engage in diverse interactions including hydrogen bonding, coordination bonding, and van der Waals forces. These interactions facilitate

stable binding with carbon molecules, heavy metals, and pollutants [49]. Such chemical adsorption is generally more stable than physical adsorption, contributing to enhanced long-term carbon fixation in soil environments. Beyond adsorption, functional groups govern sequestration performance. Carboxyl and hydroxyl groups enhance hydrophilicity and cation exchange, improving CO_2 retention and soil stability; carbonyl and phenolic groups facilitate redox reactions, stabilizing carbon–mineral complexes. Modification strategies further optimize functionality: alkaline activation increases carboxyl/phenolic groups, oxidation promotes carbonyl/carboxyl groups, nitrogen doping introduces pyridinic/pyrrolic sites that strengthen CO_2 binding, and metal impregnation (e.g., Fe, Mg) forms catalytic complexes enhancing conversion and stability. Collectively, these modifications extend biochar's carbon persistence. Polar functional groups like carboxyl and hydroxyl groups can improve the hydrophilicity and surface charge distribution of biochar in soil, thereby increasing its cation exchange capacity (CEC). These indirect factors further influence carbon sequestration efficiency [20].

Modification of biochar through chemical and physical processes can enhance its surface properties, significantly improving CO_2 adsorption capacity [50]. KOH activation increases micropore volume and introduces more carboxyl and phenolic hydroxyl groups, while H_3PO_4 treatment tends to incorporate phosphate-containing groups, improving phosphorus availability and indirectly enhancing soil carbon fixation capacity. Strategies such as nitrogen doping, metal loading, and redox modification are increasingly applied in biochar modification. These methods regulate electronic structures and promote chemical reactions between CO_2 molecules and surface groups, thereby achieving more efficient and stable carbon fixation [2].

High-temperature pyrolysis (600-700 ℃) typically results in extensive removal of volatile components from biomass, endowing the resulting biochar with higher degrees of aromatization, graphitization, and structural stability [3]. This highly aromatic structure is less susceptible to microbial decomposition in the environment, thereby exhibiting longer carbon residence time. In contrast, although low-temperature pyrolysis (300-400 ℃) retains more surface-active functional groups, enhancing cation

exchange capacity (CEC) and nutrient retention capabilities, its relatively loose carbon structure is prone to oxidation or microbial degradation. This compromises its long-term carbon sequestration effectiveness [51]. Collectively, specific surface area and functional groups constitute the structural foundation and chemical reactivity core of biochar in carbon sequestration applications. Optimizing feedstock selection, regulating pyrolysis temperature, introducing hierarchical pore structures, and applying modification techniques can substantially enhance carbon sequestration efficiency and environmental adaptability. Therefore, practical biochar applications require comprehensive consideration of structural characteristics, reactivity, stability, and soil-climate conditions for targeted optimization and regulation.

3 Carbon Sequestration Benefits of Biochar Carbon for Different Applications

3.1 Carbon substitution potential in Steelmaking

The steel industry is a pillar of the global economy. In this context, biomass-derived char (often termed charcoal in metallurgical practice, but referred to here consistently as biochar for comparability) has attracted attention as a renewable carbon source. Fossil fuels account for nearly three-quarters of energy input in steel production, and their extensive use results in substantial CO_2 emissions. Approximately 1.9 tons of CO_2 are released per ton of steel produced [52], contributing to 7%-9% of global energy system carbon emissions [53]. Under the dual-carbon goals, the low-carbon development of the steel industry faces significant challenges. As a renewable carbon source, biochar offers a novel solution for carbon emission reduction in this sector due to its low production-related carbon emissions and potential to substitute fossil fuels. In blast furnace Steelmaking, biochar application can reduce reliance on coal and coke. Compared to conventional coal, biochar exhibits higher volatile matter content, larger specific surface area, and lower carbon structural order. These properties shift the combustion curve toward higher-temperature zones in blast furnaces, thereby improving combustion efficiency and reducing carbon emissions [54]. Furthermore, the combustion process of biochar can absorb atmospheric CO_2, creating a carbon neutrality effect that effectively mitigates CO_2 emissions during Steelmaking [44]. In

sintering processes, replacing part of conventional carbon sources (coke breeze or coal powder) with biochar reduces multiple pollutant emissions. At a 10% substitution ratio, SOx emissions decrease; when substitution increases to 40%, NOx and CO_2 emissions are also reduced. However, in practical applications, the rapid combustion rate of biochar makes sustained stable combustion difficult to maintain over extended periods. This may cause sintering temperatures to drop in high-temperature zones, necessitating careful control of biochar substitution ratios [55].

Practical evidence supports biochar as a steelmaking substitute. In Brazil, charcoal-based biochar has long replaced coke in pig iron production [56]. Rio Tinto's BioIron™ pilot in Australia achieved up to 95% CO_2 reduction using biomass-derived biochar with renewable hydrogen and electricity [52]. Smaller-scale trials (5-10% substitution in sintering or coal injection) also reduced emissions without impairing furnace performance. These cases demonstrate both technical feasibility and scalability of biochar as a low-carbon fuel replacement.

From a life cycle perspective, the application of biochar in blast furnace Steelmaking can significantly reduce greenhouse gas emissions. The global warming potential (GWP) of the biochar-integrated blast furnace Steelmaking process is 2054.00 kg CO_2-eq, representing a reduction of 420.61 kg CO_2-eq compared to conventional processes [57]. Rio Tinto's BioIron™ R&D facility in Western Australia has established a low-carbon Steelmaking process that integrates fast-growing biomass with renewable energy and carbon cycling. This approach may reduce carbon emissions by up to 95% compared to traditional blast furnace methods [52]. This demonstrates that biochar application not only reduces fossil fuel consumption but also effectively mitigates carbon emissions throughout the Steelmaking process. Biochar utilization can further improve other environmental indicators in blast furnace operations. For instance, compared to conventional Steelmaking, biochar addition significantly reduces acidification potential (AP), eutrophication potential (EP), and non-carcinogenic health impact potential. These improvements in environmental metrics underscore the critical importance of biochar implementation for achieving sustainable development in the steel industry.

The application of biochar in blast furnace Steelmaking begins with a series of preprocessing stages—including biomass collection, transportation, drying, and grinding—followed by slow pyrolysis to produce biochar. This process consumes resources such as electricity, diesel fuel, and water while generating emissions and byproducts. The resulting biochar is then utilized in blast furnace Steelmaking (Figure 3) [42]. The carbon footprint analyses for steelmaking and construction follow a standardized lifecycle assessment, covering processes from feedstock to end-of-life. Emissions and sequestration data were normalized per ton of product (steel or concrete) using the GWP100 metric, and harmonized from literature sources under consistent boundary conditions to ensure reproducibility. As shown in Figure 3, the system boundary includes raw material preprocessing, pyrolysis conversion, and downstream substitution of fossil carbon in the furnace, ensuring full life-cycle accounting of carbon flows. It substitutes for conventional fossil fuels, enhances combustion efficiency, optimizes reaction kinetics, and generates synergistic effects with other materials. These mechanisms effectively reduce carbon emissions in the Steelmaking process, providing a viable solution for low-carbon transition in the steel industry and advancing its trajectory toward green and sustainable development.

Fig. 3. System boundary and material flow MPB scenario [46].

3.2 Application of carbon sequestration in building materials

Construction-based industries contribute significantly to global CO_2 emissions across various manufacturing processes. When incorporated into this sector, biomass-derived char is usually treated simply as a carbonaceous additive; here we consistently retain the umbrella term biochar, while discussing specifications unique to building materials. Cement production alone accounts for 7% of total global CO_2 emissions during its production, processing, and preparation stages [58]. Incorporating biochar into building materials not only enhances material performance but also achieves substantial carbon capture and sequestration, supporting carbon reduction goals [59]. In concrete applications, studies have added peanut shell biochar at incorporation rates of 1%-5%. Results demonstrate that BC500 and BC700 significantly enhance mechanical properties at optimal incorporation rates of 5% and 3%, respectively. Concurrently, BC500 and BC700 achieve carbon sequestration capacities of 541 kg CO_2-eq and 980 kg CO_2-eq, respectively [42]. Another study designed carbon-negative core-shell aggregates with biochar cores and cement-based shells via cold-bonding methods. Carbon emission assessments reveal that producing one ton of these aggregates emits only 69 kg CO_2, significantly lower than commercial sintered aggregates [43].

Life cycle assessment and cost-benefit analysis demonstrate that biochar as concrete aggregate enhances mechanical strength and successfully achieves carbon-negative concrete production, sequestering 59 kg CO_2 per ton [60]. Utilizing biochar derived from agricultural waste to partially replace cement paste—at a substitution rate of 5 wt%—effectively promotes carbonation, achieving 10.2% CO_2 absorption after 28 days[61]. Incorporating biochar into super sulfated cement accelerates hydration, increasing compressive and flexural strength by 16.2% and 28.9%, respectively, while reducing the system's global warming potential (GWP) to 53.3 kg·CO_2·eq/m^3. This approach provides insights for developing near-zero or carbon-negative construction materials[62]. Combining modified biochar with multi-source solid waste enables the

development of novel cold-bonded artificial lightweight aggregates (CALAs) with high carbon sequestration performance and negative carbon footprints. Adding 3 wt% modified biochar significantly improves CALAs' physical and mechanical properties, accelerates mineralization reaction rates, and achieves negative carbon emissions—exhibiting 14.56 wt% CO_2 absorption with an emission intensity of 76.7 kg CO_2/t. Throughout the aggregate's life cycle, substantial negative carbon effects are realized, offering a sustainable alternative for artificial aggregates with dual CO_2 emission reduction and capture capabilities [63]. Replacing 5% cement with biochar fills concrete pores, resulting in a denser microstructure while enhancing compressive and splitting tensile strength. Although 10% biochar incorporation provides greater carbon sequestration capacity, it may slightly compromise mechanical performance. Low temperatures adversely affect concrete properties; nevertheless, biochar-integrated shotcrete shows developmental potential for enhancing buildings overall carbon sequestration performance [64].

The carbonation process of biochar in concrete is illustrated in Figure 4. This schematic highlights both the role of biochar pores in storing water and CO_2, and its participation in forming stable carbonates during hydration. During the mixing process, biochar absorbs a portion of water and stores it within its pores. Throughout the concrete curing period, this free water is gradually released, promoting the hydration reaction process. Concurrently, CO_2 diffuses into the interior of the concrete through the pores of the cementitious matrix. Biochar also provides active sites for CO_2 adsorption. The CO_2 dissolves in the pore solution within both the concrete and the biochar in its liquid phase. Finally, the dissolved carbon dioxide interacts with substances produced during hydration, such as $Ca(OH)_2$ and C-S-H, forming compounds like $CaCO_3$ [64].

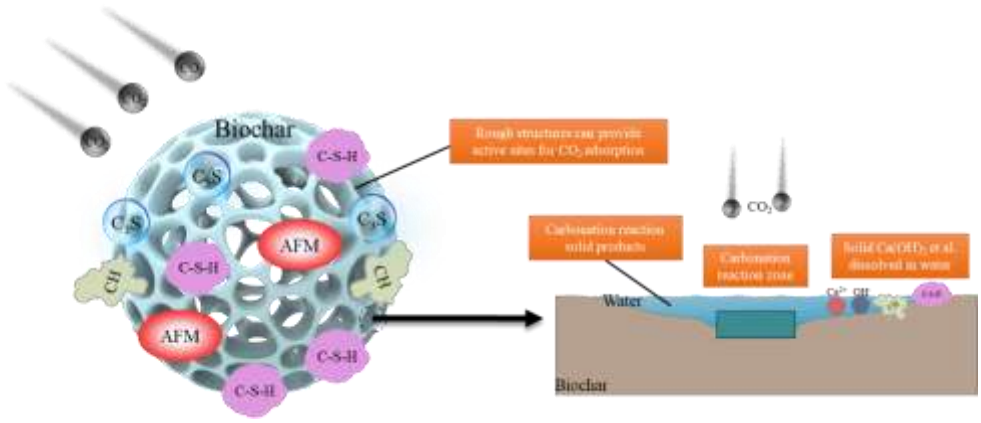

Fig. 4. Schematic diagram of carbon sequestration process of biochar in concrete [64].

Current research indicates that the application of biochar in cement-based construction materials demonstrates significant potential for carbon sequestration and performance enhancement. Through the optimization of incorporation rate (typically 1%-5%), pyrolysis temperature (500-700 °C), and modification processes, biochar can not only improve the material's mechanical strength, reduce porosity, and enhance durability, but also achieve a carbon-negative effect via carbon mineralization and substitution of carbon-intensive raw materials. However, the balance between biochar incorporation level and material performance, the influence of pyrolysis conditions on structural stability, and the efficiency of carbon fixation under long-term environmental exposure still require further investigation.

3.3 Carbon sequestration efficiency in agricultural soil

The addition of biochar to soil can improve soil conditions and increase plant biomass, thereby reducing greenhouse gas emissions. In this application, the narrower definition of biochar as a soil amendment coincides with our terminology, so no further distinction is required. During the production of biochar, approximately 50% of the initial carbon is retained within the biochar. Annual soil application of biochar could offset up to nearly 12% of total global CO_2 emissions, potentially serving as a long-term solution for global CO_2 emission reduction [8]. The biochar-induced reduction effects on CO_2 and CH_4 primarily stem from its microporous structure, alkaline

constituents, and extensive adsorption effects. As the pyrolysis temperature increases, the surface adsorption capacity of biochar is enhanced, leading to stronger adsorptive protection of soil organic matter by the biochar [65].

The carbon sequestration efficiency of biochar in soil is influenced by multiple factors, including its physicochemical properties, application rate, soil type, and management practices [49]. Due to its highly aromatic carbon structure and resistance to decomposition, biochar can significantly increase soil organic carbon (SOC) stocks. In agricultural systems, biochar alters the agricultural carbon flow pathway, encompassing input substitution, process regulation, and ultimately output suppression (Figure 5). Applying biochar at 20-40 t·ha^{-1} can increase SOC content by 26.3%-29.8%[66]. In a wheat-maize rotation experiment, SOC increased by 141.8% one year after biochar application [67]. High-dose application (40 t·ha^{-1}) of straw-derived biochar is more conducive to SOC accumulation [66].

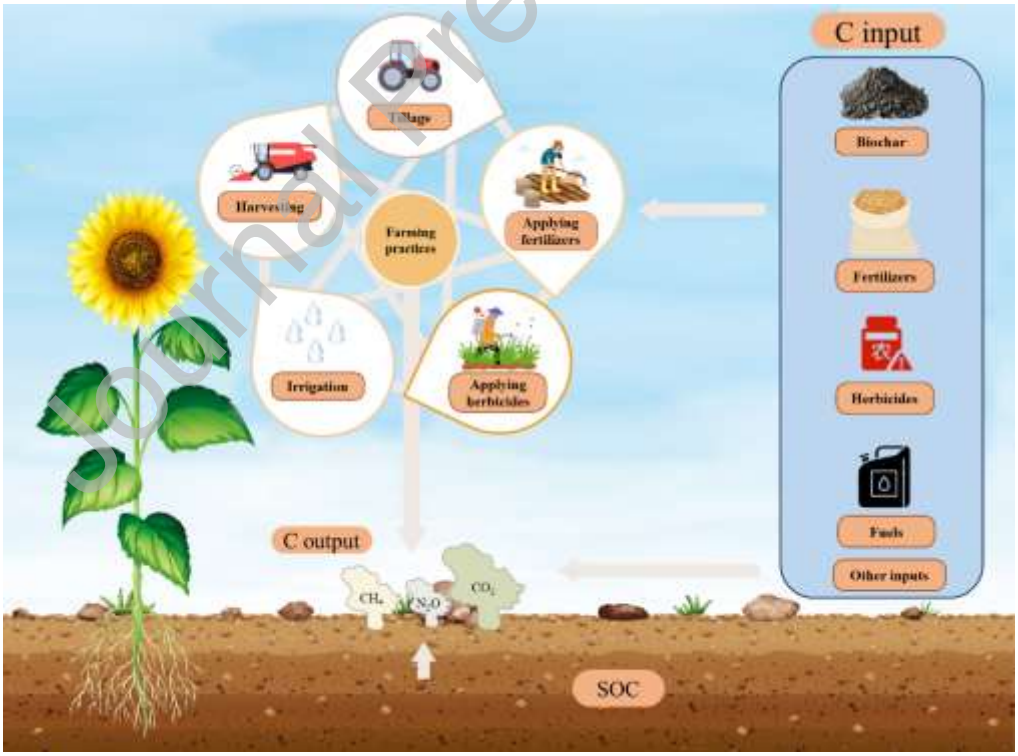

Fig. 5. System boundary for calculating GHG emissions in the sunflower cropping system [68].

Through the adsorption of greenhouse gases (CO_2, CH_4) and the suppression of soil organic carbon mineralization, biochar can indirectly reduce carbon emissions. In farmland within a freeze-thaw region, consecutive application of biochar at 30 $t \cdot ha^{-1}$ for two years resulted in an average annual carbon emission reduction of 16.7% [69]. In saline-alkali soil, biochar combined with specific tillage practices reduced the net global warming potential (NGWP) by 12660.4-43431.9 kg CO_2-eq$\cdot ha^{-1}$ [68]. The southeastern United States, due to its abundant biomass resources and significant yield increase effects, represents an economically optimal region for biochar application [70]. In saline-alkali soil, the contribution of biochar to carbon sequestration is higher than that of conventional straw return [68]. In semi-arid farmland, biochar combined with biodegradable plastic film significantly increased carbon use efficiency (CUE) by 26.93% while reducing the net GWP by 7.08% [71]. Under intermittent alternate wetting and drying irrigation (IAWD) in paddy fields, biochar application decreased the net GWP to -23.0 t CO_2-eq$\cdot ha^{-1}$ and increased SOC stocks by 56.9 t $C \cdot ha^{-1}$, with synergistic effects significantly superior to those under continuous flooding conditions [72]. Application of acid-modified biochar (HBC) in soybean fields within black soil regions increased soil organic matter by 42.57%, reduced greenhouse gas emission intensity, and enhanced net ecosystem economic benefit (NEEB) by 57.86% [73].

Biochar may help mitigate climate impacts associated with land-use change and enhance carbon sequestration in soil. Future research needs to focus on the challenges of scaling up production, such as balancing biomass collection radius and carbon footprint, alongside the trade-off inherent in high-temperature pyrolysis, which enhances stability but reduces nutrient availability. Simultaneously, research should optimize biochar modification techniques (magnetization, bio-activation) and application strategies tailored to specific soil-climate conditions to balance carbon sequestration with agricultural sustainability goals [74].

4 Predictive modeling of biochar carbon sequestration performance

4.1 Feature database construction

In multiple studies, machine learning models widely adopt pyrolysis parameters (pyrolysis temperature, heating rate, residence time) and feedstock properties (volatile matter, ash content, fixed carbon, and C/H/O/N ratios) as input features. Li et al. constructed a database encompassing 10 input variables, including the proximate analysis of the feedstock (fixed carbon, volatile matter, ash), ultimate analysis (C, H, O, N), and pyrolysis conditions (temperature PT, heating rate HR, residence time RT), to predict biochar yield and its elemental composition [75]. Furthermore, Tee et al. highlighted the influence of pyrolysis conditions and the proximate and ultimate analysis of biomass on biochar specific surface area and yield. They noted that the ultimate composition of the feedstock has a greater impact on BET specific surface area, while the proximate composition significantly influences yield [76]. Wang et al. utilized ML to predict the capabilities of biochar in areas such as pollutant adsorption and heavy metal removal [77].

Although many factors influence biochar's sequestration potential, this analysis focused on quantifiable indicators (TC, VM, Ash, Yield) and process parameters (temperature, heating rate, residence time). Due to the challenges in quantifying biomass type, we opted to use other measurable indicators (such as Total Carbon (TC), Volatile Matter (VM), Fixed Carbon (FC), and Specific Surface Area (SSA)) as indirect representations of biomass type. These indicators reflect the main components and properties of the biomass and are more feasible for modeling purposes. Two aspects were excluded due to data gaps but merit acknowledgement. First, cellulose-hemicellulose-lignin composition strongly shapes pyrolysis: cellulose/hemicellulose decompose at lower temperatures with high volatile release and low char yield, whereas lignin enhances aromatic stability and long-term retention. Yet standardized cellulose data linked to sequestration indices are scarce. Second, pyrolysis atmosphere affects char structure and carbon retention, but most studies report only temperature and residence time, with atmosphere conditions seldom standardized. Both factors are

qualitatively noted here and should be incorporated once broader datasets enable robust modeling.

We compiled and organized references relevant to biochar carbon sequestration. For references not explicitly addressing carbon sequestration, estimates were made based on the following calculation method: the net carbon sequestration of 1 kg biochar is equivalent to 1.41 kg CO_2 [78]. This conversion factor is used to account for carbon emission reductions at the application stage when such data are not explicitly provided in the literature. It enables consistency in the calculation of carbon sequestration across different studies, particularly when application-specific carbon reductions are not reported.

The summarized data are presented in Table 4 to facilitate model construction and validation. This dataset comprises seven elements: columns 1 to 6 are predictor variables, and column 7 (carbon sequestration rate) is the response variable. These six predictor variables are: pyrolysis temperature (TP), total carbon content (TC), fixed carbon content (FC), volatile matter content (VM), ash content (Ash), and specific surface area (SSA). These parameters were selected because they collectively characterize key physicochemical properties of biochar (pyrolysis temperature determines pore structure evolution; TC, FC, VM, and Ash reflect carbon matrix composition characteristics; SSA indicates surface active sites) and its pyrolysis transformation mechanisms. Analyzing these predictors based on the carbon sequestration rate aids in establishing a multifactorial coupling model. This model reveals the quantitative relationships between biochar stability and feedstock properties/preparation conditions, thereby providing a scientific basis for feedstock screening, process optimization, and long-term carbon sequestration efficacy assessment in carbon sequestration applications. The dataset used for modeling was comprehensively evaluated to ensure completeness and consistency across different feedstocks and pyrolysis conditions. The predictive analysis explicitly quantifies the relationships between CS and the governing parameters—TC, FC, VM, Ash, SSA, and TP. Random forest and neural network models were implemented to capture complex nonlinear dependencies among these variables, while multiple linear regression

provided an interpretable baseline for comparison. The ensemble models demonstrated strong predictive capability and allowed identification of dominant variables influencing CS performance, thereby establishing a robust multivariate framework for assessing carbon sequestration dynamics across diverse application scenarios.

Table 4

Characterization database.

TP(°C)	TC (%)	FC (%)	VM (%)	Ash (%)	SSA(m^2/g)	CS (%)	References
280	73.17	49.88	47.93	2.19	11.18	22.53	[44]
500	80.91	64.49	34.09	1.42	15.43	8.45	[79]
260	69.72	47.68	51.11	1.21	9.43	33.80	[45]
220	56.50	21.53	74.88	3.59	1.95	56.33	[80]
400	72.79	61.53	30.65	6.28	47.40	45.06	[46]
600	79.20	63.36	25.94	4.20	25.90	19.15	[81]
210	60.32	21.06	74.76	1.56	2.53	16.90	[82]
240	63.95	39.95	58.21	1.84	1.36	12.39	[47]
500	43.70	14.70	17.20	67.50	21.90	12.50	[15]
500	42.70	40.20	11.00	48.40	47.40	34.17	[15]
500	52.10	18.90	26.60	53.80	13.30	16.07	[15]
500	24.20	10.50	11.00	77.60	113.00	8.93	[15]
500	26.60	20.60	15.80	61.90	71.60	17.51	[15]
500	56.00	16.40	30.00	53.50	133.00	13.94	[15]
500	75.80	72.00	17.50	9.94	203.00	61.20	[15]
500	62.10	59.20	18.90	20.80	3.33	50.32	[15]
500	62.90	63.70	17.60	18.00	33.20	54.15	[15]
500	73.70	72.90	16.00	10.60	43.50	61.97	[15]
500	39.30	17.40	29.30	52.60	2.78	14.79	[15]
500	25.60	3.84	32.40	63.50	3.78	3.26	[15]
200	37.00	12.60	50.70	35.70	3.59	10.71	[15]
300	39.10	34.70	27.40	37.20	4.26	29.50	[15]
400	42.70	40.20	11.00	48.40	47.40	34.17	[15]
500	45.30	19.20	10.70	69.60	42.40	16.32	[15]
200	38.70	22.50	70.20	7.21	2.53	19.13	[15]
300	59.80	53.20	31.30	14.70	3.48	45.22	[15]
400	62.90	63.70	17.60	18.00	33.20	54.15	[15]
500	68.90	72.10	11.10	16.20	182.00	61.29	[15]
300	65.80	52.64	39.80	7.55	12.13	34.15	[14]
500	75.25	60.20	29.89	9.90	17.48	23.09	[14]
700	77.44	61.95	26.94	11.10	27.43	21.88	[14]
300	63.78	51.02	40.87	8.09	11.09	37.63	[14]
500	72.67	58.13	30.48	11.37	19.06	25.83	[14]

TP(°C)	TC (%)	FC (%)	VM (%)	Ash (%)	SSA(m^2/g)	CS (%)	References
700	77.57	62.05	25.19	12.75	597.01	22.25	[14]
300	51.56	41.24	43.26	15.48	10.05	47.89	[14]
500	55.61	44.48	28.36	27.14	35.61	22.69	[14]
700	57.55	46.04	24.03	29.92	121.00	19.54	[14]
300	57.31	45.84	36.31	17.83	4.51	31.79	[14]
500	60.63	48.50	28.95	22.54	7.52	21.98	[14]
700	62.61	50.08	25.94	23.96	25.92	19.67	[14]
500	76.80	53.10	16.00	10.60	7.53	43.02	[42]
700	83.40	55.80	31.30	14.70	36.50	14.84	[42]
700	61.95	37.85	58.21	1.84	124.70	9.70	[60]
500	79.50	69.60	18.30	12.80	477.00	11.29	[43]
500	56.60	56.60	35.70	1.80	7.53	13.85	[83]
500	73.40	75.00	15.40	9.60	141.00	12.27	[63]
800	62.61	50.08	25.94	23.96	37.47	6.53	[62]
400	68.92	55.13	60.32	4.56	3.72	17.32	[84]
500	52.12	41.69	41.26	16.48	8.35	14.24	[85]
450	57.55	46.04	23.03	28.92	11.34	11.04	[68]
500	50.69	40.55	40.26	15.48	34.47	13.79	[73]

(TP, Temperature; TC, Total Carbon; FC, Fixed Carbon; VM, Volatile Matter; CS, Carbon Sequestration.)

4.2 Multiple linear regression model

In the field of biochar carbon sequestration research, understanding the key factors influencing the CS is crucial for optimizing biochar production and enhancing carbon sequestration efficiency. By fitting a multiple linear regression (MLR) model, the influence of each variable on the target variable was quantified, thereby revealing the intrinsic relationships among factors within complex systems [86]. Based on the data in Table 4, an MLR model for predicting the CS was fitted.

The MLR provides a transparent baseline: TC and FC are positively associated with CS, VM and Ash are negative, while SSA shows a weak positive effect. Analysis of the heatmap and multiple linear regression model (Figure 6) revealed significant correlations between the biochar CS and multiple variables. The model exhibited strong goodness-of-fit ($R^2 = 0.91$), enabling effective prediction of variations in carbon sequestration. Analysis based on correlation coefficients indicated a combined influence of various parameters on biochar carbon sequestration. Among these, TC and

FC were identified as key positive influencing factors, showing weak (r = 0.22) and significant (r = 0.47) positive correlations with CS, respectively. Additionally, specific surface area (SSA) exerted a weak positive influence on carbon sequestration (r = 0.28).

Conversely, VM and Ash negatively impacted carbon sequestration, exhibiting negative correlations with CS (r = -0.24 and r = -0.23, respectively). The negative correlation between ash content and CS can be attributed to the fact that higher ash content often corresponds to lower carbon content in biochar. Ash, being inorganic, does not contribute to the carbon sequestration potential of biochar, and high levels of ash can reduce biochar stability and carbon retention capacity. Therefore, ash content indirectly hinders long-term carbon sequestration, as biochar with higher ash content tends to have a lower overall carbon fixation capability.

Within the correlation relationships, TC was highly positively correlated with FC (r = 0.83), while TC was negatively correlated with VM (r = -0.53), and FC was also negatively correlated with VM (r = -0.68). This suggests that increasing TC and FC contributes to reducing VM, thereby benefiting carbon sequestration. Simultaneously, SSA was negatively correlated with VM (r = -0.28), indicating that reducing VM may help increase SSA, consequently enhancing carbon sequestration. Therefore, to optimize carbon sequestration effectiveness, priority should be given to enhancing TC, FC, and Yield, while controlling the content of VM and Ash to mitigate their negative impacts.

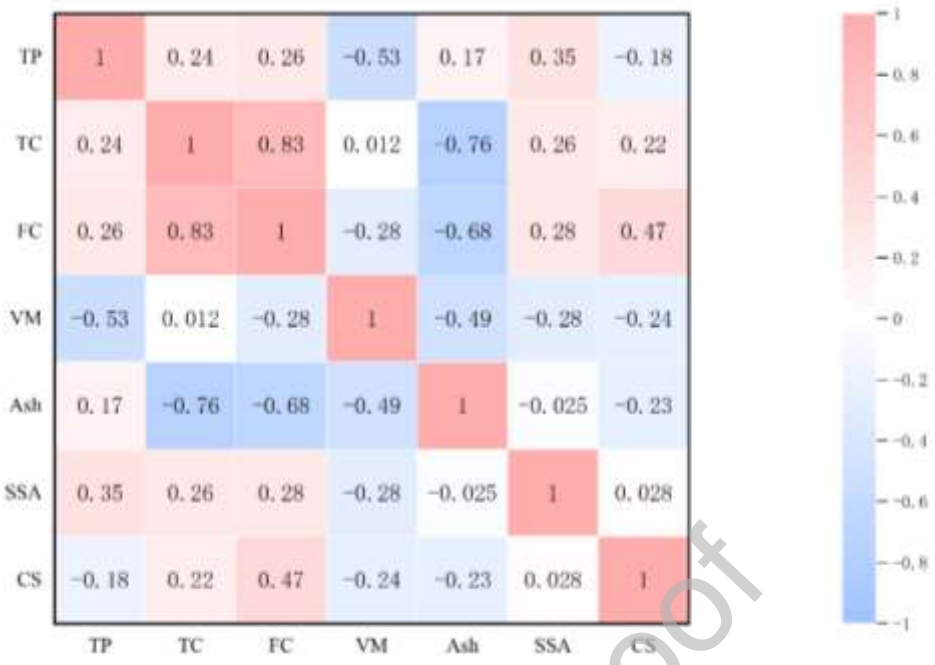

Fig. 6. Multiple Linear Regression Heatmap.

4.3 Random forest model

Random Forest (RF) is an ensemble model based on decision trees. It creates multiple decision trees using random subsets of data and aggregates predictions through voting or averaging to enhance generalization and prevent overfitting. Its advantage lies in the ability to automatically evaluate feature importance [87]. Wang et al. pointed out that RF is not only suitable for prediction but can also identify the degree of influence of input variables on the outcome, such as the dominant role of pyrolysis temperature on Yield [77]. Tee et al. employed Garson's algorithm and the connection weight approach to analyze feature importance, revealing that volatile matter (VM) and fixed carbon (FC) are the primary factors influencing biochar Yield [76].

We utilized the data from Table 4 to train a Random Forest (RF) model for predicting the carbon sequestration rate (CS). To enhance model performance, we performed feature engineering on the data, creating interaction features and polynomial features to capture more complex patterns and relationships within the data. Subsequently, based on the feature importance evaluation provided by the RF model, we conducted feature selection, retaining only features with importance higher than the

average value. This reduced the feature dimensionality and lowered the model's complexity and risk of overfitting. Following feature selection, we employed grid search to optimize and adjust the model's key parameters. The number of decision trees (numTrees) was set to 300 to balance model complexity and computational cost. The two parameters adjusted were MinLeafSize and NumPredictorsToSample, with the value range for MinLeafSize being [1, 5, 10] and for NumPredictorsToSample being [2, 3, 4, 5, 6]. To evaluate the model performance more accurately, we used cross-validation to assess both the base model and the model after feature selection based on feature importance. Ultimately, on the training set, the RF model after feature selection and parameter optimization demonstrated good predictive performance, achieving a training MAE of 6.35 and a testing MAE of 10.85. This indicates that the model can fit the training data well and possesses strong predictive capability (Figure 7).

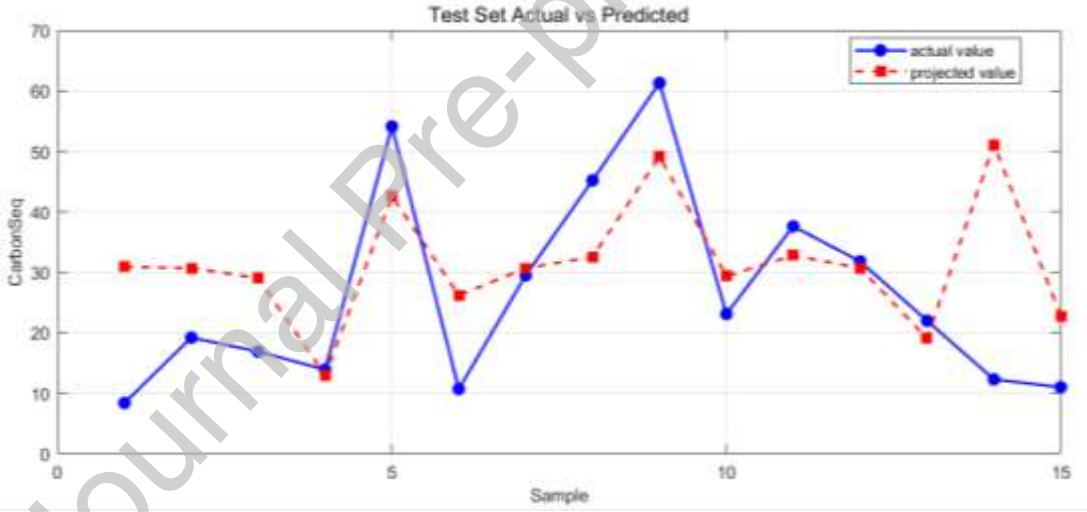

Fig. 7. Comparison of Random Forest training model and testing model.

4.4 Neural network model

Artificial Neural Networks (ANNs) exhibit distinct advantages in predicting complex nonlinear multivariate processes, particularly in scenarios involving carbon sequestration rate (CS) prediction. Even without prior knowledge of the correlations between input and output variables, neural networks can achieve effective prediction by learning underlying patterns within the data [76]. Although the dataset is limited (~50 samples), it is sufficient for exploratory ANN modeling using a simple network

architecture and early stopping. Within the field of biochar research, numerous ANN-based models have been applied to various directions. Li et al. employed Bayesian optimization for hyperparameter tuning and enhanced network generalization based on cross-validation [75]. Tee et al. utilized a feedforward neural network trained with the Levenberg-Marquardt algorithm, optimizing the number of hidden layers and neurons through trial-and-error, which effectively mitigated overfitting [76].

The neural network training results employing the Levenberg-Marquardt algorithm indicated that the model achieved the minimum gradient (1e-7) at epoch 41, leading to early stopping before reaching the maximum epoch limit of 1000. The optimizer reduced the gradient from 2.41 to 7.94e-11, decreased the performance metric from 0.826 to 7.85e-21, and lowered the Mu value from 0.001 to 1e-9. The training process required merely 4 seconds, demonstrating good convergence and high efficiency. Analysis of variable importance using Partial Dependence Plots (PDPs) revealed that temperature (TP) exhibited a significant negative correlation with carbon sequestration (CS). The CS value decreased substantially within the 300-600 °C range, identifying TP as a key regulatory factor. The influence of specific surface area (SSA) was relatively stable, showing noticeable fluctuation at low values and plateauing after exceeding 100 m^2 /g (Figure 8).

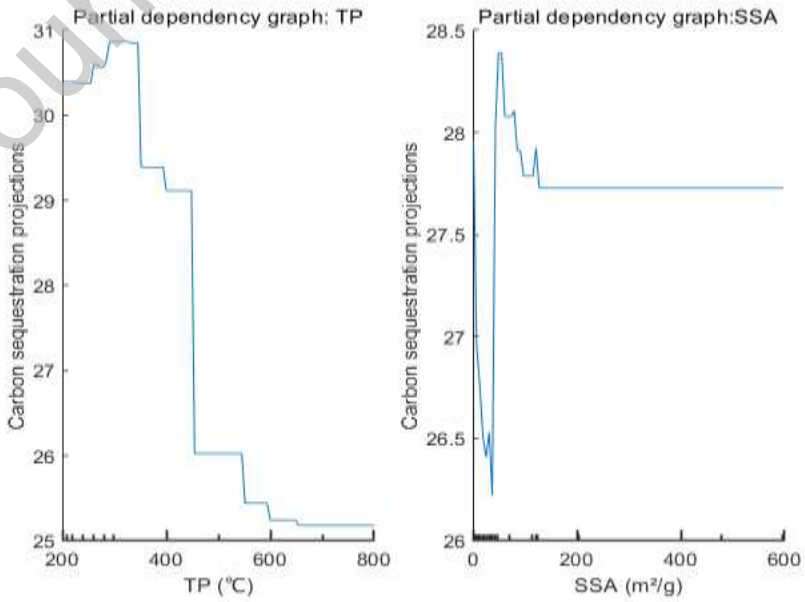

Fig. 8. Bias dependence analysis of temperature and specific surface area.

The prediction comparison on the test set revealed scatter points deviating from the ideal 1:1 line with the presence of outliers, yielding a low R^2 value of only 0.53. This indicates that the model's predictions were less accurate for some data points (Figure 9). The potential causes may include the limited size of the test set (only approximately 50 samples), complex interactions between features not being adequately captured, and limited generalization capability. Subsequent research needs to encompass: expanding the sample size, optimizing feature engineering (incorporating pH, ash content, etc.), adjusting the model architecture (attempting deeper architectures or ensemble learning), and handling outliers, aiming to enhance overall model performance.

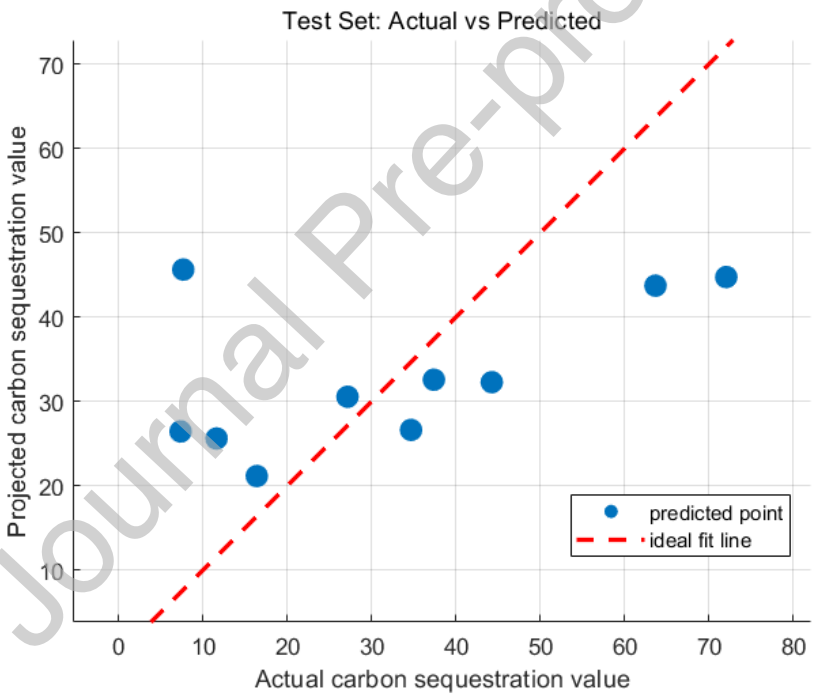

Fig. 9. Neural Network Training Models and Testing Models.

5 Conclusions and outlook

This review analyzed carbon emission regulation during biochar preparation, assessed sequestration benefits across steelmaking, construction, and soil applications, and established a machine learning-based predictive model for carbon sequestration

rate (CS). Results show that feedstock properties and pyrolysis conditions critically shape sequestration efficiency: high-carbon, low-ash feedstocks processed at 500-600 °C with 120-180 min residence times yield superior CS performance. Regression results highlight Yield and TC as primary drivers, while SSA, VM, and Ash exert secondary influences. Applications confirm biochar's potential to reduce the carbon footprint by >20%, enhance SOC storage, and deliver carbon-negative effects, underscoring its role as a negative emission technology.

Despite progress, challenges remain in long-term stability, multi-objective optimization, and predictive model generalizability. In particular, the moderate performance of the neural network model ($R^2 = 0.53$) indicates that larger and more diverse datasets incorporating additional physicochemical parameters are required to fully capture the nonlinear relationships governing carbon sequestration. Priority should be given to four directions: (1) developing sector-specific standards and testing protocols for steelmaking, construction, and soils; (2) conducting long-term, multi-climate field trials with standardized monitoring, reporting, and verification (MRV) systems; (3) optimizing pyrolysis processes and co-feeding strategies alongside risk management for PAHs and heavy metals; and (4) integrating open datasets, machine learning, and techno-economic assessments to enable industrial scale-up and credible carbon crediting. Taken together, these priorities highlight that biochar is positioned as a scalable negative emission pathway, contingent upon systematic resolution of these research gaps.

CRediT authorship contribution statement

Pin lv: Writing – original draft, Visualization, Data curation, Conceptualization.
Qun Huan: Writing – review & editing, Validation, Data curation.
Min Song: Writing – review & editing, Validation, Supervision, Funding acquisition.

Declaration of Competing Interest

The authors declare that they have no known competing financial interests or personal relationships that could have appeared to influence the work reported in this paper.

Acknowledgments

This work was supported by the National Science Fund for Excellent Young Scholars (No. 52222609)

Data availability

No data was used for the research described in the article.

References

[1] A. Slameršak, G. Kallis, D.W. O'Neill, Energy requirements and carbon emissions for a low-carbon energy transition, Nat. Commun. 13 (2022) 6932. https://doi.org/10.1038/s41467-022-33976-5.

[2] Sri Shalini S., Palanivelu K., Ramachandran A., V. Raghavan, Biochar from biomass waste as a renewable carbon material for climate change mitigation in reducing greenhouse gas emissions—a review, Biomass Convers. Biorefin. 11 (2021) 2247–2267. https://doi.org/10.1007/s13399-020-00604-5.

[3] P. Ye, B. Guo, H. Qin, C. Wang, Y. Liu, Y. Chen, P. Bian, D. Lu, L. Wang, W. Zhao, Y. Yang, L. Hong, P. Gao, P. Ma, B. Zhan, Q. Yu, The state-of-the-art review on biochar as green additives in cementitious composites: performance, applications, machine learning predictions, and environmental and economic implications, Biochar 7 (2025) 21–51. https://doi.org/10.1007/s42773-024-00423-1.

[4] C. Wilson, A. Grubler, N. Bento, S. Healey, S. De Stercke, C. Zimm, Granular technologies to accelerate decarbonization, Science 368 (2020) 36–39. https://doi.org/10.1126/science.aaz8060.

[5] F. Qin, C. Zhang, G. Zeng, D. Huang, X. Tan, A. Duan, Lignocellulosic biomass carbonization for biochar production and characterization of biochar reactivity, Renew. Sustain. Energy Rev. 157 (2022) 112056. https://doi.org/10.1016/j.rser.2021.112056.

[6] S. Yu, J. He, Z. Zhang, Z. Sun, M. Xie, Y. Xu, X. Bie, Q. Li, Y. Zhang, M. Sevilla, M.-M. Titirici, H. Zhou, Towards negative emissions: hydrothermal carbonization of biomass for sustainable carbon materials, Adv. Mater. 36 (2024) 0–44. https://doi.org/10.1002/adma.202307412.

[7] G. Ravindiran, S. Rajamanickam, G. Janardhan, G. Hayder, A. Alagumalai, O. Mahian, S.S. Lam, C. Sonne, Production and modifications of biochar to engineered materials and its application for environmental sustainability: a review, Biochar 6 (2024) 62–89. https://doi.org/10.1007/s42773-024-00350-1.

[8] T.A. Kurniawan, M.H.D. Othman, X. Liang, H.H. Goh, P. Gikas, K.-K. Chong, K.W. Chew, Challenges and opportunities for biochar to promote circular economy and carbon neutrality, J. Environ. Manage. 332 (2023) 117429. https://doi.org/10.1016/j.jenvman.2023.117429.

[9] A. Cowie, Biochar as a fast track to net zero, Nat. Food 4 (2023) 203–204. https://doi.org/10.1038/s43016-023-00714-z.

[10] J. Lehmann, E. Barrios, M. Devault, L. Li, R. Nelson, J. Six, J. Trimmer, Biochar in the circular bionutrient economy, Proc. Natl. Acad. Sci. U. S. A. 122 (2025). https://doi.org/10.1073/pnas.2503668122.

[11] X. Deng, F. Teng, M. Chen, Z. Du, B. Wang, R. Li, P. Wang, Exploring negative emission potential of biochar to achieve carbon neutrality goal in China, Nat. Commun. 15 (2024). https://doi.org/10.1038/s41467-024-45314-y.

[12] L. Luo, J. Wang, J. Lv, Z. Liu, T. Sun, Y. Yang, Y.-G. Zhu, Carbon Sequestration Strategies in Soil Using Biochar: Advances, Challenges, and Opportunities, Environ. Sci. Technol. 57 (2023) 11357–11372. https://doi.org/10.1021/acs.est.3c02620.

[13] J. Yu, M. Song, Z. Li, Optimization of biochar preparation process and carbon sequestration effect of pruned wolfberry branches, Green Process. Synth. 11 (2022) 423–434. https://doi.org/10.1515/gps-2022-0044.

[14] S. Ding, Z. Lan, S. Fang, Pyrolysis temperature determines the amendment effects of poplar

residue-derived biochars on reducing CO_2 emission, Gcb Bioenergy 15 (2023) 1030–1045. https://doi.org/10.1111/gcbb.13080.

[15] W. Liu, H. Jiang, H. Yu, Development of biochar-based functional materials: toward a sustainable platform carbon material, Chem. Rev. 115 (2015) 12251–12285. https://doi.org/10.1021/acs.chemrev.5b00195.

[16] A.K. Varma, R. Shankar, P. Mondal, A review on pyrolysis of biomass and the impacts of operating conditions on product yield, quality, and upgradation, in: P.K. Sarangi, S. Nanda, P. Mohanty (Eds.), Recent Advancements in Biofuels and Bioenergy Utilization, Springer Singapore, Singapore, 2018: pp. 227–259. https://doi.org/10.1007/978-981-13-1307-3_10.

[17] S. Fawzy, A.I. Osman, H. Yang, J. Doran, D.W. Rooney, Industrial biochar systems for atmospheric carbon removal: a review, Environ. Chem. Lett. 19 (2021) 3023–3055. https://doi.org/10.1007/s10311-021-01210-1.

[18] A.I. Osman, S. Fawzy, M. Farghali, M. El-Azazy, A.M. Elgarahy, R.A. Fahim, M.I.A.A. Maksoud, A.A. Ajlan, M. Yousry, Y. Saleem, D.W. Rooney, Biochar for agronomy, animal farming, anaerobic digestion, composting, water treatment, soil remediation, construction, energy storage, and carbon sequestration: a review, Environ. Chem. Lett. 20 (2022) 2385–2485. https://doi.org/10.1007/s10311-022-01424-x.

[19] X. Zhao, H. Zhou, V.S. Sikarwar, M. Zhao, A.-H.A. Park, P.S. Fennell, L. Shen, L.-S. Fan, Biomass-based chemical looping technologies: the good, the bad and the future, Energy Environ. Sci. 10 (2017) 1885–1910. https://doi.org/10.1039/C6EE03718F.

[20] Y. Xie, L. Wang, H. Li, L.J. Westholm, L. Carvalho, E. Thorin, Z. Yu, X. Yu, Ø. Skreiberg, A critical review on production, modification and utilization of biochar, J. Anal. Appl. Pyrolysis 161 (2022) 105405. https://doi.org/10.1016/j.jaap.2021.105405.

[21] R.M. Jayaraju, K. Gaddam, G. Ravindiran, S. Palani, M.P. Paulraj, A. Achuthan, P. Saravanan, S.K. Muniasamy, Biochar from waste biomass as a biocatalyst for biodiesel production: an overview, Appl. Nanosci. 12 (2022) 3665–3676. https://doi.org/10.1007/s13204-021-01924-2.

[22] R.K. Mishra, K. Mohanty, A review of the next-generation biochar production from waste biomass for material applications, Science of The Total Environment 904 (2023) 167171. https://doi.org/10.1016/j.scitotenv.2023.167171.

[23] S. Jung, J.-H. Kim, D.-J. Lee, K.-Y.A. Lin, Y.F. Tsang, M.-H. Yoon, E.E. Kwon, Virtuous utilization of biochar and carbon dioxide in the thermochemical process of dairy cattle manure, Chem. Eng. J. 416 (2021) 129110. https://doi.org/10.1016/j.cej.2021.129110.

[24] S.K. Das, G.K. Ghosh, R. Avasthe, Applications of biomass derived biochar in modern science and technology, Environ. Technol. Innovation 21 (2021) 101306. https://doi.org/10.1016/j.eti.2020.101306.

[25] J. Lu, H. Li, Y. Zhang, Z. Liu, Nitrogen migration and transformation during hydrothermal liquefaction of livestock manures, ACS Sustainable Chem. Eng. 6 (2018) 13570–13578. https://doi.org/10.1021/acssuschemeng.8b03810.

[26] S. Yu, X. Yang, P. Zhao, Q. Li, H. Zhou, Y. Zhang, From biomass to hydrochar: Evolution on elemental composition, morphology, and chemical structure, J. Energy Inst. 101 (2022) 194–200. https://doi.org/10.1016/j.joei.2022.01.013.

[27] L. Zhao, X. Cao, O. Mašek, A. Zimmerman, Heterogeneity of biochar properties as a function of feedstock sources and production temperatures, J. Hazard. Mater. 256–257 (2013) 1–9. https://doi.org/10.1016/j.jhazmat.2013.04.015.

[28] H. Wang, R. Srinivasan, F. Yu, P. Steele, Q. Li, B. Mitchell, Effect of acid, alkali, and steam explosion pretreatments on characteristics of bio-oil produced from pinewood, Energy Fuels 25 (2011) 3758–3764. https://doi.org/10.1021/ef2004909.

[29] Y.-F. Huang, P.-T. Chiueh, W.-H. Kuan, S.-L. Lo, Microwave pyrolysis of lignocellulosic biomass: heating performance and reaction kinetics, Energy 100 (2016) 137–144. https://doi.org/10.1016/j.energy.2016.01.088.

[30] E. Henrich, N. Dahmen, F. Weirich, R. Reimert, C. Kornmayer, Fast pyrolysis of lignocellulosics in a twin screw mixer reactor, Fuel Process. Technol. 143 (2016) 151–161. https://doi.org/10.1016/j.fuproc.2015.11.003.

[31] R.J.M. Westerhof, D.Wim.F. Brilman, M. Garcia-Perez, Z. Wang, S.R.G. Oudenhoven, S.R.A. Kersten, Stepwise fast pyrolysis of pine wood, Energy Fuels 26 (2012) 7263–7273. https://doi.org/10.1021/ef301319t.

[32] X. Zhao, J. Zhang, Z. Song, H. Liu, L. Li, C. Ma, Microwave pyrolysis of straw bale and energy balance analysis, J. Anal. Appl. Pyrolysis 92 (2011) 43–49. https://doi.org/10.1016/j.jaap.2011.04.004.

[33] H. Nan, J. Yin, F. Yang, Y. Luo, L. Zhao, X. Cao, Pyrolysis temperature-dependent carbon retention and stability of biochar with participation of calcium: implications to carbon sequestration, Environ. Pollut. 287 (2021) 117566. https://doi.org/10.1016/j.envpol.2021.117566.

[34] S.K. Hoekman, A. Broch, L. Felix, W. Farthing, Hydrothermal carbonization (HTC) of loblolly pine using a continuous, reactive twin-screw extruder, Energy Convers. Manage. 134 (2017) 247–259. https://doi.org/10.1016/j.enconman.2016.12.035.

[35] P.V. Nidheesh, A. Gopinath, N. Ranjith, A. Praveen Akre, V. Sreedharan, M. Suresh Kumar, Potential role of biochar in advanced oxidation processes: A sustainable approach, Chem. Eng. J. 405 (2021) 126582. https://doi.org/10.1016/j.cej.2020.126582.

[36] J.-S. Lu, Y. Chang, C.-S. Poon, D.-J. Lee, Slow pyrolysis of municipal solid waste (MSW): a review, Bioresour. Technol. 312 (2020) 123615. https://doi.org/10.1016/j.biortech.2020.123615.

[37] P. Thomas, C.W. Lai, M.R. Bin Johan, Recent developments in biomass-derived carbon as a potential sustainable material for super-capacitor-based energy storage and environmental applications, J. Anal. Appl. Pyrolysis 140 (2019) 54–85. https://doi.org/10.1016/j.jaap.2019.03.021.

[38] L. Leng, Q. Xiong, L. Yang, H. Li, Y. Zhou, W. Zhang, S. Jiang, H. Li, H. Huang, An overview on engineering the surface area and porosity of biochar, Science of The Total Environment 763 (2021) 144204. https://doi.org/10.1016/j.scitotenv.2020.144204.

[39] K. Kameyama, T. Miyamoto, Y. Iwata, The Preliminary Study of Water-Retention Related Properties of Biochar Produced from Various Feedstock at Different Pyrolysis Temperatures, Materials 12 (2019) 1732. https://doi.org/10.3390/ma12111732.

[40] S.S.A. Alkurdi, I. Herath, J. Bundschuh, R.A. Al-Juboori, M. Vithanage, D. Mohan, Biochar versus bone char for a sustainable inorganic arsenic mitigation in water: what needs to be done in future research?, Environ. Int. 127 (2019) 52–69. https://doi.org/10.1016/j.envint.2019.03.012.

[41] V. Dhyani, T. Bhaskar, A comprehensive review on the pyrolysis of lignocellulosic biomass, Renewable Energy 129 (2018) 695–716. https://doi.org/10.1016/j.renene.2017.04.035.

[42] Y. Zhang, Y. Maierdan, T. Guo, B. Chen, S. Fang, L. Zhao, Biochar as carbon sequestration material combines with sewage sludge incineration ash to prepare lightweight concrete, Constr. Build. Mater. 343 (2022) 128116. https://doi.org/10.1016/j.conbuildmat.2022.128116.

[43] S. Zou, M.L. Sham, J. Xiao, L.M. Leung, J.-X. Lu, C.S. Poon, Biochar-enabled carbon negative

aggregate designed by core-shell structure: a novel biochar utilizing method in concrete, Constr. Build. Mater. 449 (2024) 138507. https://doi.org/10.1016/j.conbuildmat.2024.138507.
[44] W. Liang, Y. Cui, D. Zhu, Y. Chen, Y. Han, L. Yue, C. Jiang, R. Xu, X. Ning, J. Zhang, C. Wang, G. Wang, Co-combustion reaction of corn stalk hydrochar and anthracite: Kinetics, mechanism and CO2 emission reduction, Fuel 388 (2025) 134470. https://doi.org/10.1016/j.fuel.2025.134470.
[45] J. Li, R. Xu, G. Wang, J. Zhang, B. Song, W. Liang, C. Wang, Study on the feasibility and co-combustion mechanism of mixed injection of biomass hydrochar and anthracite in blast furnace, Fuel 304 (2021) 121465. https://doi.org/10.1016/j.fuel.2021.121465.
[46] M. Yang, Q. Peng, G. Cao, X. Tao, Y. Chang, X. Jiang, Feasibility analysis and environmental impact evaluation of biochar derived from mango pit for blast furnace injection, Chem. Eng. J. 487 (2024) 150451. https://doi.org/10.1016/j.cej.2024.150451.
[47] G. Wang, R. Li, J. Dan, X. Yuan, J. Shao, J. Liu, K. Xu, T. Li, X. Ning, C. Wang, Preparation of biomass hydrochar and application analysis of blast furnace injection, Energies 16 (2023) 0–16. https://doi.org/10.3390/en16031216.
[48] G. Kwon, A. Bhatnagar, H. Wang, E.E. Kwon, H. Song, A review of recent advancements in utilization of biomass and industrial wastes into engineered biochar, J. Hazard. Mater. 400 (2020) 123242. https://doi.org/10.1016/j.jhazmat.2020.123242.
[49] M. Marcińczyk, P. Oleszczuk, Biochar and engineered biochar as slow- and controlled-release fertilizers, J. Cleaner Prod. 339 (2022) 130685. https://doi.org/10.1016/j.jclepro.2022.130685.
[50] P.D. Dissanayake, S. You, A.D. Igalavithana, Y. Xia, A. Bhatnagar, S. Gupta, H.W. Kua, S. Kim, J.-H. Kwon, D.C.W. Tsang, Y.S. Ok, Biochar-based adsorbents for carbon dioxide capture: A critical review, Renew. Sustain. Energy Rev. 119 (2020) 109582. https://doi.org/10.1016/j.rser.2019.109582.
[51] G. Kwon, D.-W. Cho, D.C.W. Tsang, E.E. Kwon, H. Song, One step fabrication of carbon supported cobalt pentlandite (Co9S8) via the thermolysis of lignin and Co3O4, J. Co2 Util. 27 (2018) 196–203. https://doi.org/10.1016/j.jcou.2018.07.016.
[52] T.R. Sarker, D.Z. Ethen, S. Nanda, Decarbonization of metallurgy and steelmaking industries using biochar: a review, Chem. Eng. Technol. 47 (2024) 0–12. https://doi.org/10.1002/ceat.202400217.
[53] H. Na, J. Sun, Z. Qiu, Y. Yuan, T. Du, Optimization of energy efficiency, energy consumption and CO2 emission in typical iron and steel manufacturing process, Energy 257 (2022) 124822. https://doi.org/10.1016/j.energy.2022.124822.
[54] G. Wang, J. Zhang, J. Shao, Z. Liu, G. Zhang, T. Xu, J. Guo, H. Wang, R. Xu, H. Lin, Thermal behavior and kinetic analysis of co-combustion of waste biomass/low rank coal blends, Energy Convers. Manage. 124 (2016) 414–426. https://doi.org/10.1016/j.enconman.2016.07.045.
[55] W. Tan, B. Xi, Toward carbon emission reduction in steel production by substituting pulverized coal and coke with biochar, ACS Es&t Eng. 4 (2024) 1253–1255. https://doi.org/10.1021/acsestengg.4c00151.
[56] J. Massuque, M.D. Roque Lima, P.H. Müller Da Silva, T. De Paula Protásio, P.F. Trugilho, Potential of charcoal from non-commercial Corymbia and Eucalyptus wood for use in the steel industry, Renewable Energy 211 (2023) 179–187. https://doi.org/10.1016/j.renene.2023.04.061.
[57] W. Liang, G. Wang, R. Xu, X. Ning, J. Zhang, X. Guo, C. Jiang, C. Wang, Life cycle assessment of blast furnace ironmaking processes: A comparison of fossil fuels and biomass hydrochar applications, Fuel 345 (2023) 128138. https://doi.org/10.1016/j.fuel.2023.128138.

[58] R. Mensah, V. Shanmugam, S. Narayanan, N. Razavi, A. Ulfberg, T. Blanksvärd, F. Sayahi, P. Simonsson, B. Reinke, M. Försth, G. Sas, D. Sas, O. Das, Biochar-Added Cementitious Materials—A Review on Mechanical, Thermal, and Environmental Properties, Sustainability 13 (2021) 9336. https://doi.org/10.3390/su13169336.

[59] J. Liu, G. Liu, W. Zhang, Z. Li, F. Xing, L. Tang, Application potential analysis of biochar as a carbon capture material in cementitious composites: a review, Constr. Build. Mater. 350 (2022) 128715. https://doi.org/10.1016/j.conbuildmat.2022.128715.

[60] L. Chen, Y. Zhang, L. Wang, S. Ruan, J. Chen, H. Li, J. Yang, V. Mechtcherine, D.C.W. Tsang, Biochar-augmented carbon-negative concrete, Chem. Eng. J. 431 (2022) 133946. https://doi.org/10.1016/j.cej.2021.133946.

[61] R. Agarwal, N. Pawar, Supriya, P. Rawat, D. Rai, R. Kumar, S. Naik B, Thermo-mechanical behavior of cementitious material with partial replacement of Class-II biochar with Accelerated Carbonation Curing (ACC), Ind. Crops Prod. 204 (2023) 117335. https://doi.org/10.1016/j.indcrop.2023.117335.

[62] S. Xiao, Y. Li, C. Xu, J. Deng, L. Cheng, H. Zhang, Y. Zhou, J. Hong, The influence of biochar addition on the mechanical performance, hydration mechanism, and carbonation capacity of super sulfated cement, Constr. Build. Mater. 463 (2025) 140073. https://doi.org/10.1016/j.conbuildmat.2025.140073.

[63] B. Yan, Y. Hu, Q. Huan, Z. Liu, J. Lai, S. Wang, M. Song, Optimal regulation of modified biochar in solid waste-derived lightweight aggregates: enhancing carbonation mechanisms and negative carbon emissions, Chem. Eng. J. 508 (2025). https://doi.org/10.1016/j.cej.2025.160920.

[64] G. Liu, L. Liu, H. Liu, H. Zheng, Investigating CO2 sequestration properties of biochar shotcrete, Constr. Build. Mater. 443 (2024) 137779. https://doi.org/10.1016/j.conbuildmat.2024.137779.

[65] L. Wang, D. Chen, L. Zhu, Biochar carbon sequestration potential rectification in soils: Synthesis effects of biochar on soil CO2, CH4 and N2O emissions, Science of The Total Environment 904 (2023) 167047. https://doi.org/10.1016/j.scitotenv.2023.167047.

[66] J. Zhang, H. Sun, J. Ma, X. Zhang, C. Wang, S. Zhou, Effect of straw biochar application on soil carbon, greenhouse gas emissions and nitrogen leaching: A vegetable crop rotation field experiment, Soil Use Manage. 39 (2023) 729–741. https://doi.org/10.1111/sum.12877.

[67] D. He, H. Ma, D. Hu, X. Wang, Z. Dong, B. Zhu, Biochar for sustainable agriculture: Improved soil carbon storage and reduced emissions on cropland, J. Environ. Manage. 371 (2024) 123147. https://doi.org/10.1016/j.jenvman.2024.123147.

[68] M. Hu, Z. Qu, Y. Li, Y. Xiong, G. Huang, Contrasting effects of different straw return modes on net ecosystem carbon budget and carbon footprint in saline-alkali arid farmland, Soil Tillage Res. 239 (2024) 106031. https://doi.org/10.1016/j.still.2024.106031.

[69] R. Zhang, Evaluating annual soil carbon emissions under biochar-added farmland subjecting from freeze-thaw cycle, J. Environ. Manage. (2024) 0–12.

[70] J. Dumortier, H. Dokoohaki, A. Elobeid, D.J. Hayes, D. Laird, F.E. Miguez, Global land-use and carbon emission implications from biochar application to cropland in the United States, Journal of Cleaner Production 258 (2020) 120684. https://doi.org/10.1016/j.jclepro.2020.120684.

[71] Y. Wang, Z. Tian, X. Li, M. Zhang, Y. Fang, Y. Xiang, Y. Liu, E. Liu, Z. Jia, K.H.M. Siddique, W. Ting, W. Zhang, P. Zhang, Straw-derived biochar regulates soil enzyme activities, reduces greenhouse gas emissions, and enhances carbon accumulation in farmland under mulching, Field

Crops Res. 317 (2024) 109547. https://doi.org/10.1016/j.fcr.2024.109547.
[72] C. Liu, T. Chen, F. Zhang, H. Han, B. Yi, D. Chi, Soil carbon sequestration increment and carbon-negative emissions in alternate wetting and drying paddy ecosystems through biochar incorporation, Agric. Water Manage. 300 (2024) 108908. https://doi.org/10.1016/j.agwat.2024.108908.
[73] Y. Gong, R. Hou, Q. Fu, T. Li, J. Wang, Z. Su, W. Shen, W. Zhou, Y. Wang, M. Li, Modified biochar reduces the greenhouse gas emission intensity and enhances the net ecosystem economic budget in black soil soybean fields, Soil Tillage Res. 237 (2024) 105978. https://doi.org/10.1016/j.still.2023.105978.
[74] X. Wang, T. Zou, J. Lian, Y. Chen, L. Cheng, Y. Hamid, Z. He, P. Jeyakumar, X. Yang, H. Wang, Simultaneous mitigation of cadmium contamination and greenhouse gas emissions in paddy soil by iron-modified biochar, J. Hazard. Mater. 488 (2025) 137430. https://doi.org/10.1016/j.jhazmat.2025.137430.
[75] Y. Li, R. Gupta, W. Li, Y. Fang, J. Toney, S. You, Machine learning-assisted life cycle assessment of biochar soil application, J. Cleaner Prod. 498 (2025) 145109. https://doi.org/10.1016/j.jclepro.2025.145109.
[76] J.X. Tee, A. Selvarajoo, S.K. Arumugasamy, Prediction of carbon sequestration of biochar produced from biomass pyrolysis by artificial neural network, J. Environ. Chem. Eng. 10 (2022) 107640. https://doi.org/10.1016/j.jece.2022.107640.
[77] W. Wang, J.-S. Chang, D.-J. Lee, Machine learning applications for biochar studies: a mini-review, Bioresour. Technol. 394 (2024) 130291. https://doi.org/10.1016/j.biortech.2023.130291.
[78] S. Gupta, Carbon sequestration in cementitious matrix containing pyrogenic carbon from waste biomass: A comparison of external and internal carbonation approach, J. Build. Eng. 43 (2021) 102910. https://doi.org/10.1016/j.jobe.2021.102910.
[79] E. Yustanti, E.Y. Wardhono, A.T. Mursito, A. Alhamidi, Types and composition of biomass in biocoke synthesis with the coal blending method, Energies 14 (2021) 0–18. https://doi.org/10.3390/en14206570.
[80] G. Wang, J. Zhang, J.-Y. Lee, X. Mao, L. Ye, W. Xu, X. Ning, N. Zhang, H. Teng, C. Wang, Hydrothermal carbonization of maize straw for hydrochar production and its injection for blast furnace, Appl. Energy 266 (2020) 114818. https://doi.org/10.1016/j.apenergy.2020.114818.
[81] E. Mousa, K. Sjöblom, Modeling and Optimization of Biochar Injection into Blast Furnace to Mitigate the Fossil CO2 Emission, Sustainability 14 (2022) 2393. https://doi.org/10.3390/su14042393.
[82] S. Ye, S. Hao, C. Yan, X. Zhang, Y. Di, X. Zhou, H. Zhang, Z. Jiang, X. Zhang, Optimization of microalgal hydrothermal carbonization parameters using the response surface method for biochar applications in blast furnaces to reduce carbon emissions, Fuel 381 (2025) 133671. https://doi.org/10.1016/j.fuel.2024.133671.
[83] T. Wang, Y. Tang, S. Qin, G. Li, H. Wu, C.K.Y. Leung, Sustainable and mechanical properties of engineered cementitious composites with biochar: integrating micro- and macro-mechanical insight, Cem. Concr. Compos. 155 (2025) 105813. https://doi.org/10.1016/j.cemconcomp.2024.105813.
[84] T. E, C. Ji, Y. Cheng, S. Yang, L. Chen, D. Wang, Y. Wang, Y. Li, Effect of waste leather dander biochar on soil organic carbon sequestration, J. Environ. Chem. Eng. 12 (2024) 112633. https://doi.org/10.1016/j.jece.2024.112633.

[85] J. Pang, Z. Tian, M. Zhang, Y. Wang, T. Qi, Q. Zhang, E. Liu, W. Zhang, X. Ren, Z. Jia, K.H.M. Siddique, P. Zhang, Enhancing carbon sequestration and greenhouse gas mitigation in semiarid farmland: The promising role of biochar application with biodegradable film mulching, J. Integr. Agric. (2023) S2095311923004586. https://doi.org/10.1016/j.jia.2023.12.011.
[86] A. Li, Y. Li, X. Wang, S. Li, J. Chang, F. Liao, H. Gao, H. Fu, Y. Zhang, J. Zhang, Y. Liao, Exploration of iodine adsorption sites on porous biochar derived from silkworm excrement through structural regulation, linear fitting, multiple linear regression analysis, and DFT calculations, Colloids Surf., A 720 (2025) 137136. https://doi.org/10.1016/j.colsurfa.2025.137136.
[87] S. Uppalapati, P. Paramasivam, N. Kilari, J.S. Chohan, P.K. Kanti, H. Vemanaboina, L.H. Dabelo, R. Gupta, Precision biochar yield forecasting employing random forest and XGBoost with Taylor diagram visualization, Sci. Rep. 15 (2025) 7105. https://doi.org/10.1038/s41598-025-91450-w.

Graphical Abstract:

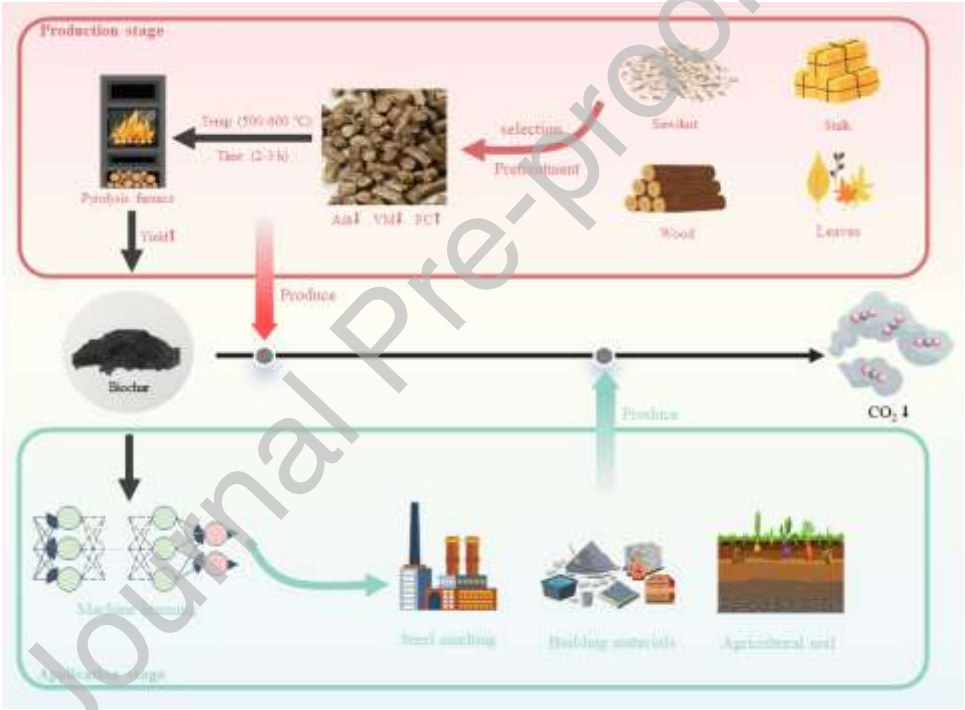

Declaration of interests

The authors declare that they have no known competing financial interests or personal relationships that could have appeared to influence the work reported in this paper.